Journal of Materials Chemistry A

ROYAL SOCIETY OF CHEMISTRY

PAPER

View Article Online
View Journal | View Issue

Check for updates

Cite this: J. Mater. Chem. A, 2024, 12, 31195

Balancing Ge de-intercalation and Si re-insertion rates stabilizes hydrolytically labile germanosilicate zeolites†

Jin Zhang, ‡[a] Qiudi Yue, ‡[ab] Emad Shamma,[a] Sarra Abdi,[a] Oleg Petrov,[c] Jiří Čejka, [a] Svetlana Mintova, [b] Maksym Opanasenko *[a] and Mariya Shamzhy [a]

Germanosilicate zeolites are attractive adsorbents and catalysts, thanks to their diverse structures and versatile textural properties. However, hydrolytic instability of such zeolites, even under ambient conditions, restricts their practical applications. In this study, we report dynamic changes in the state of the zeolite framework atoms due to Ge de-intercalation and Si re-insertion in aqueous medium and propose a strategy for stabilizing zeolites with planar and orthogonal locations of Ge-rich domains by managing both processes. Adjusting the acidity or temperature of the aqueous environment enabled Ge and Si atoms to reach balanced mobility, allowing Ge atoms to be leached and Si atoms to be inserted into the released positions, thereby stabilizing the zeolite framework. The developed approach offers a practical and controllable method for structural stabilization of any labile germanosilicate material, with potential applications in catalysis, as demonstrated after the incorporation of Al-associated acid centers.

Received 7th August 2024
Accepted 16th October 2024

DOI: 10.1039/d4ta05539j

rsc.li/materials-a

Open Access Article. Published on 21 October 2024. Downloaded on 2/21/2026 7:51:59 PM.
This article is licensed under a Creative Commons Attribution 3.0 Unported Licence.

1. Introduction

Zeolites are crystalline aluminosilicate materials with well-defined micropores and are widely used as shape-selective solid acid catalysts, adsorbents, and ion exchange agents.[1] Different trivalent, tetravalent, and pentavalent elements, such as B, Fe, Ge, Ti, and P, can be introduced into silica frameworks to tune their surface chemistry and functionality.[2] Among them, Ge is an element that has opened a route to new zeolite structures with large pore sizes.[3–5] This is in particular due to the typical Ge–O–Ge bond angles in the range 120–180°, which facilitate the structural relaxation of otherwise strained small framework-building units, such as double four-rings (D4Rs). The resulting Ge-zeolites are active Lewis acid catalysts[6–8] and show interesting adsorption properties.[9,10] However, clustering of Ge atoms in D4Rs generally makes germanosilicate zeolites hydrolytically labile[11] leading to their fast deactivation due to structural collapse.[12]

The hydrolytic stability of germanosilicate zeolites is conventionally influenced by three main factors:

(i) The presence of an organic structure-directing agent (OSDA) is required for the synthesis of a zeolite. After the synthesis, OSDA stays in the voids and stabilizes the framework due to van der Waals interactions, but it needs to be removed by calcination for the practical application of a zeolite.

(ii) The number of Ge atoms per D4R – hydrolytic stability is reached when a D4R unit contains fewer than four Ge atoms on average.[13,14]

(iii) The location of these D4R units within the zeolite structure ($1D_{D4R}$, $2D_{D4R}$, or $3D_{D4R}$) – hydrolytic stability usually increases in the sequence of $1D_{D4R} < 2D_{D4R} < 3D_{D4R}$ zeolites.

$1D_{D4R}$ zeolites (for example, IWV, *CTH and ITR) have cubic units located along only one crystallographic axis, so the structure comprises silica *layers* connected by Ge-D4Rs. These zeolites can maintain their structures in OSDA-free form under ambient conditions for months, but gradually degrade upon contact with water. Conversely, $2D_{D4R}$ zeolites (such as UWY, SOV, and SOR) feature silica *chains* connected by Ge-D4R units along two orthogonal crystallographic axes. Lastly, $3D_{D4R}$ zeolites (such as IWS, POS, and -IFY) have silica clusters connected by Ge-D4R units along three mutually orthogonal directions, making them extremely sensitive to humidity. Most of these structures collapse upon OSDA removal.[15,16]

To date, two primary strategies have been developed to address the hydrolytic instability of germanosilicates by Ge depletion (Fig. 1a). The first one involves the transformation of labile germanosilicates into new zeolites by replacing Ge-rich

[a]Department of Physical and Macromolecular Chemistry, Faculty of Science, Charles University Hlavova 8, Prague 12843, Czech Republic. E-mail: maksym.opanasenko@natur.cuni.cz

[b]Laboratoire Catalyse et Spectrochimie, Normandie Université, ENSICAEN, UNICAEN, CNRS, Caen 14050, France

[c]Department of Low-Temperature Physics, Faculty of Mathematics and Physics, Charles University, V Holešovičkách 2, Prague 8 180 00, Czech Republic

† Electronic supplementary information (ESI) available. See DOI: https://doi.org/10.1039/d4ta05539j

‡ These authors contributed equally to this work.

Open Access Article. Published on 21 October 2024. Downloaded on 2/21/2026 7:51:59 PM. This article is licensed under a Creative Commons Attribution 3.0 Unported Licence.

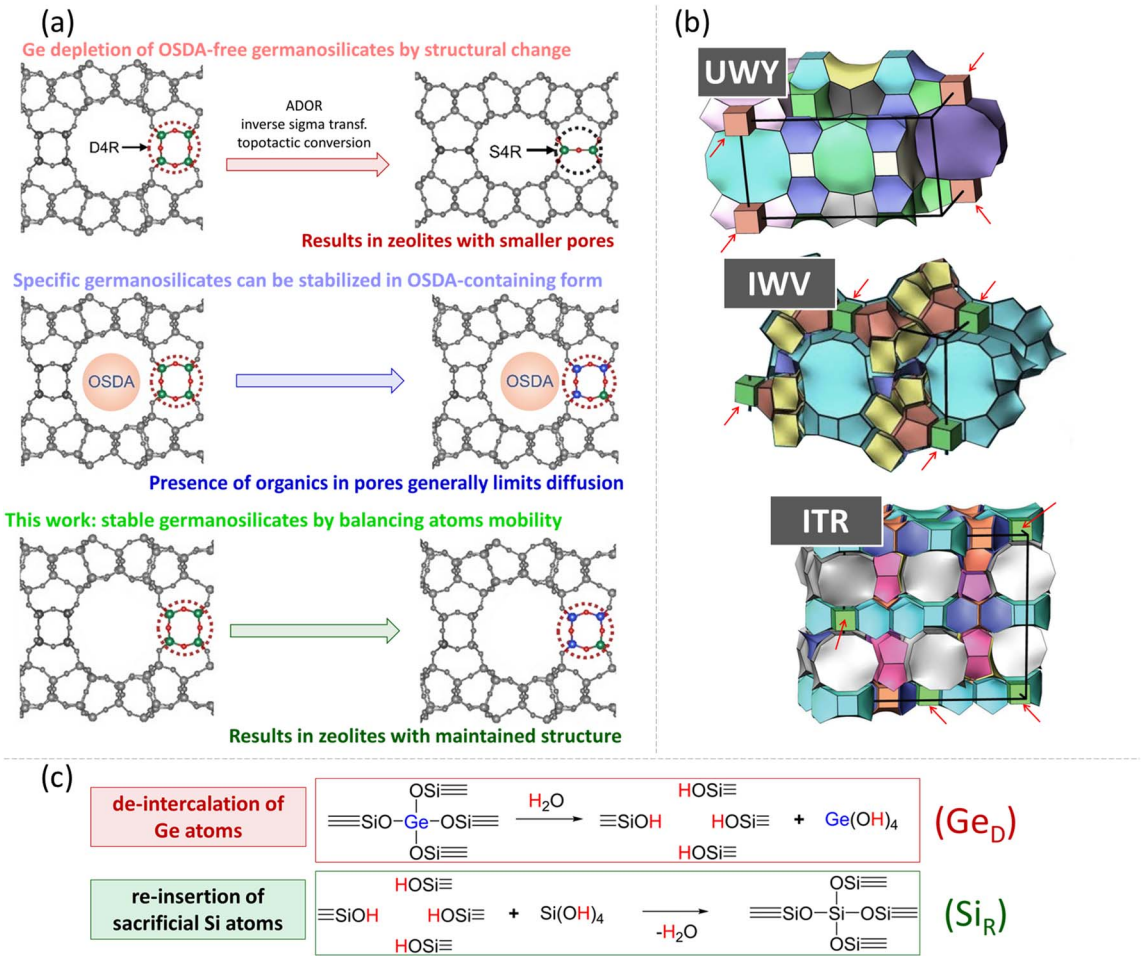

Fig. 1 (a) Schematic illustration of known methods for overcoming the hydrolytic instability of germanosilicate zeolites (structural transformation and stabilization in the OSDA-containing form) compared to the method proposed in this work. Units highlighted with dashed circles contain Ge (green), Si (blue) and O (red) atoms. (b) Examples of germanosilicate zeolites containing D4R units (highlighted with red arrows) along different crystallographic directions. (c) Simplified scheme of competing processes which occur during the treatment of germanosilicates in aqueous solutions resulting in the displacement of framework atoms. De-intercalation of Ge atoms from a zeolite framework leads to defects – silanol nests (top), while re-insertion of Si atoms into the released framework positions leads to framework reconstruction (bottom).

D4Rs with Ge-depleted –S4R–, –S4R–/O–, or –O– linkages of smaller size[17] or organic/inorganic pillars of larger size.[18,19] The second strategy involves the stabilization of OSDA-containing (otherwise labile[20,21]) $1D_{D4R}$ and $2D_{D4R}$ germanosilicate zeolites by isomorphous substitution of Ge with Si using treatment with a source of Si atoms.[20] However, these methods do not solve the important issues associated with germanosilicate zeolite stabilization: the presence of OSDA in the pores hinders the incorporation of potential heteroatoms,[22–24] while daughter zeolites produced by the structural transformation of D4Rs have micropores smaller than their parent structures.[22,25,26]

This study proposes a robust approach for structural stabilization of germanosilicate zeolites in OSDA-free form (Fig. 1b), which allows either the maintenance of their microporosity or the tailoring of hydrolytically stable zeolites with a combined system of micro- and mesopores. The proposed method is based on recent findings suggesting the competition of two processes in germanosilicate zeolite–water systems (Fig. 1c): (1) Ge atom de-intercalation from the framework, forming defects or even causing framework collapse and (2) Si atom re-insertion into the vacant positions, 'healing' the defects and preventing framework degradation.[27,28] The extent of these processes was found to depend on the treatment conditions, such as temperature, pH, and the water/zeolite ratio. Accordingly, we hypothesized that promotion of conditions for the predominance of Si re-insertion (Si_R) over Ge de-intercalation (Ge_D) could preserve the structural integrity of germanosilicate zeolites in aqueous medium and verified our hypothesis by identifying the respective conditions for the UWY framework as a typical representative of hydrolytically unstable $2D_{D4R}$ germanosilicates. Furthermore, we showed that our stabilization strategy was equally effective for $1D_{D4R}$ zeolites, such as ITR, IWV, and *CTH, thus presenting a practical method for structurally stabilizing a variety of labile germanosilicate materials.

2. Experimental methods

2.1. Synthesis

The preparation of OSDAs for the synthesis of germanosilicate zeolites UWY, IWV, ITR and *CTH as well as the procedure for

 This journal is © The Royal Society of Chemistry 2024

Open Access Article. Published on 21 October 2024. Downloaded on 2/21/2026 7:51:59 PM. This article is licensed under a Creative Commons Attribution 3.0 Unported Licence.

hydrothermal crystallization and calcination of those zeolites to remove the occluded OSDA is described in detail in the ESI.†

2.2. Stabilization

Typically, 1 g of the OSDA-free zeolites was treated with 100 ml of a freshly prepared solution of hydrochloric acid (0.1–12 M) at 25 °C (referring to RT), 60 °C or 100 °C for 16 h (if another duration is not indicated). The solid was isolated by filtration, washed with anhydrous ethanol, dried at 60 °C overnight and subsequently calcined at 350 °C for 2 h at a heating rate of 1 °C min^{-1}.

2.3. Acid site incorporation

1 g of UWY-2.6 zeolite stabilized in 6 M HCl at RT for 16 h (UWY-2.6/SBZ) was treated with 100 ml of 1 M $Al(NO_3)_3$ aqueous solution at 80 °C for 96 h according to ref. 29. The aluminated sample was subsequently filtered and washed sequentially with 0.01 M HCl and deionized water and calcined at 350 °C for 2 h at a heating rate of 1 °C min^{-1}. The prepared catalyst was designated as UWY-2.6/SBZ/Al.

2.4. Characterization

The prepared materials were characterized by powder X-ray diffraction (PXRD) to analyze their phase purity and degree of crystallinity; scanning electron microscopy (SEM) to study the size and shape of the crystals; argon physisorption for the analysis of textural properties, such as micropore volume (V_{micro}), BET surface (S_{BET}) and pore size distribution; ICP-MS for the evaluation of chemical composition; ^{29}Si and ^{19}F MAS NMR and ^{1}H–^{29}Si CP/MAS NMR spectroscopy to trace the evolution in the local environment of Si and Ge atoms and FTIR spectroscopy of adsorbed pyridine to evaluate the nature and strength of acid sites after Al incorporation. The catalytic performance of the prepared Al-substituted zeolite was assessed in the acid-site-strength sensitive Friedel–Crafts benzoylation of p-xylene, yielding 2,5-dimethylbenzophenone which is used as a UV light stabilizer in plastics, cosmetics, and films. A detailed description of the characterization techniques is provided in the ESI.†

3. Results and discussion

3.1. Balancing Ge_D and Si_R rates for low-temperature stabilization of UWY zeolites: acidity

UWY is a typical $2D_{D4R}$ germanosilicate zeolite, as schematically represented in Fig. S1.† D4R units enriched in Ge[30] are propagated in both the *a* and *b* crystallographic directions, thus isolating Si-enriched chains propagating in the *c* direction. This zeolite has been previously identified as hydrolytically unstable: after coming in contact with water at 25 °C (room temperature, RT in the following text), the structure of OSDA-free UWY collapsed, and the material became amorphous.[20]

To study the relationship between chemical composition and hydrolytic stability of UWY, the Si/Ge molar ratio of the starting zeolite was varied in the range of 1.5–3, while the concentration of the HCl used for the treatment was set at 0, 0.1, 6, and 12 M.

According to the literature, phase-pure UWY zeolites can be prepared by conventional hydrothermal crystallization but only from reaction mixtures with Si/Ge ≤ 1.5, whereas decreasing the Ge concentration yields undesired zeolites phases.[30,31] To overcome this limitation and produce UWY zeolites with higher Si/Ge ratios (1.5–3), we applied a set of seeded syntheses.[32] The resulting phase-pure UWY samples had similar crystallinity in terms of the widths and relative intensities of diffraction lines (Fig. S2†). Chemical analysis revealed that the Si/Ge ratios of the zeolites (1.6, 1.9, and 2.6) correlated with the composition of the initial synthesis mixture (Si/Ge = 1.5, 2 and 3, respectively). According to the Le Bail refinement (Fig. S16†), UWY-1.6, UWY-1.9, and UWY-2.6 display similar *b* and *c* unit cell parameters, but a slight reduction along the *a*-axis is particularly noted for the Ge-poor UWY-2.6 relative to the Ge-rich UWY-1.6 (Table S1†). This difference can be attributed to the contraction of D4R units, resulting from shorter T-O linkages due to Ge-for-Si substitution.

^{19}F is a useful NMR probe to elucidate the local composition of D4R-containing zeolites, because its chemical shift strongly depends on the Ge content in the D4R units. Specifically, the unique signal at −38 ppm observed for all-silica systems was reported to split into several NMR lines in Ge-containing zeolites, with each line corresponding to F^- ions located at the center of D4R units with specific chemical compositions: −38 ppm [8Si, 0Ge], −20 ppm [7Si, 1Ge], and −10 ppm [4Si, 4Ge].[33] The ^{19}F MAS NMR spectra of fluorinated UWY samples confirmed that the majority of D4R units were enriched in Ge, regardless of the chemical composition of the UWY zeolites (Fig. S3†). All the samples showed a prominent signal at −10 ppm, attributed to [4Si, 4Ge] D4R units, accompanied by marginal signals at −20 ppm, characteristic of [7Si, 1Ge] D4Rs with isolated Ge atoms, and at −38 ppm, typical for silica [8Si, 0Ge] D4Rs.[31,33]

Although the prepared OSDA-free UWY zeolites experienced amorphization upon contact with water at RT irrespective of the Si/Ge ratio (Fig. S2†), the UWY-2.6 with the lowest Ge content maintained its crystalline structure in 6 M HCl (Fig. S4†). By contrast, UWY-1.6 and UWY-1.9 with higher Ge concentrations were unable to withstand the acid treatment under similar conditions (Fig. S5†). Suboptimal acid concentrations (0.1 or 12 M) resulted in structural changes in UWY-2.6, manifested by changes in the positions of diffraction lines. Specifically, in 6 M HCl, all XRD peaks characteristic of UWY remained unchanged, but in HCl solutions with non-optimal concentrations, the (010) and (200) diffraction lines shifted to higher angles, and the (*hkl*) peaks with $h \neq 0$, $k \neq 0$ either decreased or disappeared (Fig. S4†).

While maintaining the structural integrity, UWY-2.6 stabilized in 6 M HCl at RT showed an increased Si/Ge ratio (Table S2†), and slightly decreased micropore sizes (based on Ar physisorption, Fig. S6†). This result is in line with the replacement of Ge–O–Si and/or Ge–O–Ge bonds with shorter Si–O–Si linkages, resulting in a decrease in the unit cell parameter *a* by 0.4 Å in the stabilized sample, while the *b* and *c* parameters were

Open Access Article. Published on 21 October 2024. Downloaded on 2/21/2026 7:51:59 PM. This article is licensed under a Creative Commons Attribution 3.0 Unported Licence.

less affected (Table S1†). The stabilization treatment significantly altered neither the shape of the Ar physisorption isotherm of type-I, characteristic of microporous materials, (Fig. S6†) nor the micropore volume of the parent UWY-2.6 (0.13 *vs.* 0.12 $cm^3\ g^{-1}$, Table S2†). Furthermore, SEM images revealed the maintenance of the crystal morphology in all acid-treated samples (Fig. S7†). These results indicate that OSDA-free $2D_{D4R}$ germanosilicate UWY can retain the structural and textural integrity under optimized conditions of acid treatment. As such, these findings contradict the consensus that OSDA-free $2D_{D4R}$ germanosilicate zeolites cannot withstand aqueous media.

To demonstrate that the performed treatment increased the stability of the initially labile UWY germanosilicate, the following two-step experiment was conducted: UWY-2.6 was stabilized in 6 M HCl at RT for 20 h, and then the stabilized product with Si/Ge = 6.1 was examined in water at RT for 24 h. The XRD patterns (Fig. S8†) indicate that the structure of the stabilized UWY was preserved in aqueous medium, while the starting zeolite did not withstand the same treatment (Fig. S2†).

As such, both Ge_D and Si_R occur in germanosilicate zeolites in aqueous solutions at neutral or acidic pH.[27,28] Defects appearing upon Ge de-intercalation can be healed by subsequent Si re-insertion, while the resulting ≡Si–O–Si≡ moiety is hydrolytically more stable than the initial ≡Si–O–Ge≡ moiety. In the absence of an additional source of silicon atoms, partial sacrificial dissolution of the amorphous phase or zeolite framework has been previously reported to generate silica species contributing to the re-insertion process.[20] Both mechanisms are possible under the stabilization conditions used in this study, as a small fraction of an amorphous phase cannot be excluded in the parent zeolite samples, while the formation of structural defects and additional micropores upon harsh treatments (*vide infra*) indicates the sacrificial consumption of framework Si atoms.

3.2. Evolution of the UWY framework upon stabilization

For a time-resolved study of the UWY – 6 M HCl system, intermediates recovered at specific times were *ex situ* analyzed using XRD, ^{29}Si and ^{1}H–^{29}Si CP MAS NMR spectroscopy and ICP-MS (Fig. 2). Although no meaningful structural transformation was detected with XRD over time (Fig. 2a and S9†), the chemical composition of UWY did change continuously (Fig. 2b). Specifically, the Si/Ge ratio quickly increased from 2.6 to 4.6 after initial 2 min of the treatment (corresponding to the loss or exchange of 1.9 out of initial 5.5 Ge atoms per D4R) and then gradually increased to 6.1 in the next 48 h (an additional exchange of 0.8 Ge atoms per D4R on average). Further increasing the treatment time to 3–6 days did not increase the Si/Ge ratio (*ca.* 5.9), indicating that the de-intercalation and re-insertion processes are equilibrated.

Notably, the change in the chemical composition of the UWY framework was accompanied by the evolution of the local environment of the framework atoms (Fig. 2c–e). Due to the anisotropic environment of Si atoms in Ge-enriched D4R units and Si-enriched chains, ^{29}Si MAS NMR spectra of UWY-2.6

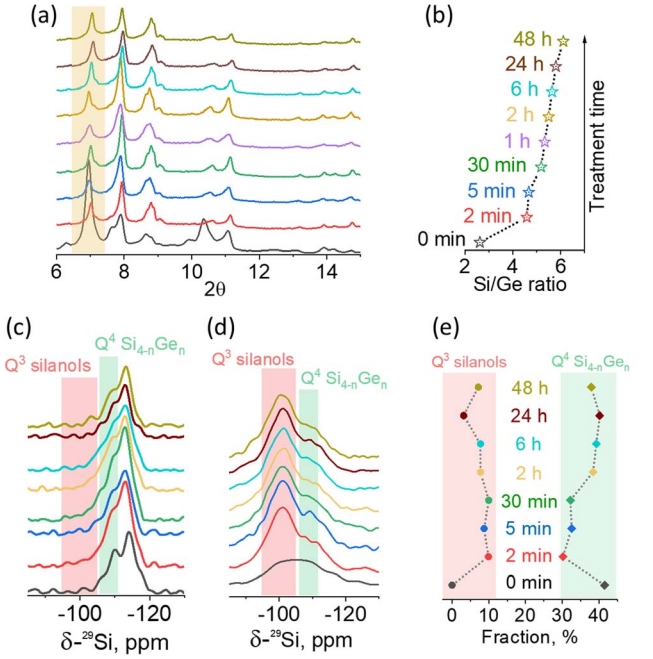

Fig. 2 Evolution of the structure, composition and state of framework atoms in OSDA-free UWY-2.6 zeolite (designated as "0 min") treated with 6 M HCl at RT for different times (2 min, 5 min, 30 min, 1 h, 2 h, 6 h, 24 h, and 48 h) followed by calcination. (a) XRD patterns (full patterns are shown in Fig. S8†). (b) Si/Ge ratio. (c) ^{29}Si MAS NMR spectra. (d) ^{1}H–^{29}Si CP MAS NMR spectra. (e) Population of Q^3 Si atoms in silanol groups (corresponding to the band at −103 ppm) and Q^4 Si atoms originating from D4R units (band at around −108 ppm). Fitting plots are shown in Fig. S10.†

revealed two types of Q^4 signals (Fig. 2c): 1) −108 ppm, assigned to Si atoms surrounded by Ge atoms in D4Rs (Q^4 $Si_{4-n}Ge_n$) and 2) −115 ppm, assigned to Si atoms surrounded by other silicon atoms in silica chains.[13,34] In acid-treated samples, an additional peak centered at −103 ppm and assigned to Q^3 Si of silanols appeared, while no Q^2 signal (usually *ca.* > −100 ppm) related to deeper hydrolysis was identified in NMR spectra (Fig. 2c). The selective enhancement of the resonance band at −103 ppm in the respective ^{1}H–^{29}Si CP MAS NMR spectra (Fig. 2d) confirms the assignment of the corresponding signal to silicon atoms coupled with the hydrogens of the hydroxyl groups through dipolar interaction in $(SiO)_3Si$–OH moieties.

The evolution of the local environment of Si atoms in UWY zeolites upon stabilization was analyzed based on the relative intensities of the signals observed in ^{29}Si MAS NMR spectra (Fig. 2e). The starting UWY contained 41% of Q^4 Si atoms in D4Rs, while their fraction decreased to 30% after immersion of the zeolite in acid solution for 2 min. Simultaneously, the fraction of defective Q^3 Si atoms increased by 10% indicating fast breaking of SiO–Ge linkages upon acid treatment. Prolonging the treatment up to 24 h resulted in gradual restoration of the Q^4 Si fraction (40%), whereas the population of Q^3 Si reached its minimum (3%). Such progressive healing of silanol defects suggests that Ge atoms are replaced by Si atoms relatively rapidly.

 This journal is © The Royal Society of Chemistry 2024

Open Access Article. Published on 21 October 2024. Downloaded on 2/21/2026 7:51:59 PM.
This article is licensed under a Creative Commons Attribution 3.0 Unported Licence.

However, prolonging the treatment for an additional 24 h (totaling 48 h of treatment time) slightly decreased the population of Q^4 Si atoms (38%) and increased the fraction of Q^3 Si (7%) without affecting the UWY structural integrity at the nanoscale level (Fig. S9†). This result suggests the existence of an optimal treatment time for a given acidity, when the zeolite structure is stabilized without forming a significant fraction of Q^3 defects. Further prolongation of the treatment apparently leads to greater deficiencies in the zeolite likely due to deeper sacrificial framework dissolution, which may potentially result in structure degradation.

3.3. Balancing Ge_D and Si_R rates for high-temperature stabilization of UWY zeolites: acidity

Under acidic conditions, isomorphous substitution of Ge for Si atoms can be facilitated at high temperatures.[20,35] Indeed, at 100 °C stabilization of the UWY structure does not require a specific acidity of 6 M HCl, but can be achieved across a range of acid concentrations (0.1–12 M) according to SEM (Fig. S11†) and XRD data analysis (Fig. S12†).

A slight right-shift of the peaks in the diffraction patterns of the stabilized UWY zeolites is in accordance with the replacement of Ge atoms by smaller Si atoms.[35] This replacement was further confirmed by chemical analysis: Si/Ge increased from 2.6 to 18.5, 26.8, and >150 after treatment at 100 °C in 0.1, 6, and 12 M HCl, respectively (Table S2†). The lack of amorphization of UWY upon high-temperature acid treatment suggests that Si_R can be further accelerated at higher temperatures.

On the other hand, compared to stabilization at RT, UWY treated with 12 M HCl at 100 °C showed a decrease in micropore volume and intensity of the diffraction peaks accompanied by the appearance of additional larger micropores, which indicates the presence of non-restored structural defects. While the size of characteristic micropores (<1 nm) was maintained suggesting successful stabilization (Fig. S13†), harsh treatments can be useful for the generation of additional micropores with sizes >1 nm and the development of additional external surface (Table S2†), the parameters considered beneficial for catalytic applications.

Acidic treatments at 100 °C were also applied to UWY-1.6 and UWY-1.9, but similar to the RT case, the UWY structure was not preserved (Fig. S14†), suggesting that Ge_D prevails over Si_R in UWY samples with relatively high Ge content, irrespective of temperature and acid concentration.

3.4. Balancing Ge_D and Si_R rates for stabilization of $1D_{D4R}$ zeolites

To assess whether the balancing of de-intercalation and re-insertion rates can be used for structural stabilization of $1D_{D4R}$ germanosilicates, zeolites with IWV, ITR, and *CTH topologies were further studied under variable conditions, similar to UWY discussed above. Selected $1D_{D4R}$ zeolites having different crystal structures and pore systems (Fig. S15†) were synthesized with a Ge content corresponding to <6 Ge atoms per 8 positions in D4R on average (Fig. 3).

The XRD patterns of $1D_{D4R}$ zeolites treated with solutions of different concentrations at different temperatures (Fig. S17 and 18†) evidence structural preservation when using 6 M HCl at 100 °C irrespective of the zeolite topology (Fig. 3). Such conditions were also found to be optimal for the structural stabilization of the $2D_{D4R}$ UWY zeolite, confirming that accelerating the mobility of framework atoms and balancing the rates of their elimination/insertion by adjustment of acid treatment is a robust method irrespective of the zeolite structure. In general, stabilized zeolites (green squares in Fig. 3) showed a minor or even negligible decrease in crystallinity with respect to the

Zeolite	UWY-1.6		UWY-1.9		UWY-2.6		IWV-4.3		IWV-5.2		ITR-2.6		CTH-4	
Pore rings	12II10x10x10						12x12				10x10x9		14x10	
D4R distribution	2D D4R						1D D4R				1D D4R		1D D4R	
Ge per D4R	7.7		6.9		5.6		7.1		6.1		~ 8		6.4	
	RT	100°C	RT	100°C	RT	100°C	RT	100°C	RT	100°C	RT	100°C	RT	100°C
-	Crystallinity degree = 100 %													
0.1 M HCl						96%								
6 M HCl					98%	99%	100%	97%	100%	94%	89%	85%		100%
12 M HCl						85%		97%		93%				100%

Fig. 3 Structural features of the studied zeolites and the summary of the treatment results. Orange squares indicate structural disordering, while green squares indicate structural preservation (the numbers represent the degree of crystallinity of the stabilized zeolites with respect to the corresponding parent germanosilicate, which was evaluated through full profile La Bail refinement, Fig. S16†).

Open Access Article. Published on 21 October 2024. Downloaded on 2/21/2026 7:51:59 PM.
This article is licensed under a Creative Commons Attribution 3.0 Unported Licence.

parent zeolites. While the increase in the Si/Ge ratio is in line with the de-intercalation of Ge from the zeolite framework, a decrease in V_{micro} and an enhancement of S_{ext}, especially in 12 M HCl, can be related to the substantial dissolution of the framework (Fig. S19 and Table S2†).

In contrast to other tested germanosilicates, *CTH zeolite did not withstand treatment with 6 M HCl at RT (Fig. 3), which can be related to the disorder in stacking of *cfi*-type layers connected by D4Rs, characteristic of this zeolite.[36] Assumedly, the tendency of *CTH for disorder can result in deceleration of the rearrangement of *cfi* layers "delaying" the restoration of a crystalline phase, especially at RT. According to the findings described in Section 3.3, applying harsher conditions (100 °C) led to the successful stabilization of *CTH. Besides, the mentioned "delay" results in an interesting collapse–restoration phenomenon revealed during a kinetic study at 100 °C (Fig. S20†). At an early stage of the treatment (0.5–2 h), the XRD patterns showed broadening and a right-shift of reflections characteristic of *CTH, indicating partial structural disorder with framework shrinkage caused by the removal of D4R units. Prolonging the treatment (>5 h) enabled restoration of *CTH with high crystallinity, albeit with slightly different positions of diffraction peaks, indicating a minor change in unit cell parameters due to the replacement of framework atoms. A similar phenomenon has been observed for UTL zeolite,[27,37] but it required the presence of additional Al ions as mobile building blocks in solution to restore the structure.

3.5. Comparative analysis of conditions affecting Ge_D and Si_R

The rates of Ge de-intercalation and Si re-insertion were proposed to depend on the acidity of the solution,[28] thus determining whether germanosilicate zeolites undergo structural collapse or maintain their structure. In dilute solutions (0.1 M HCl), the structural disordering is in line with $r(Ge_D) > r(Si_R)$, while in excessively acidic media (12 M HCl), the re-insertion of silicon fragments is hindered by fast leaching from the framework and precipitation in extraframework positions (this correlates with formation of defects mentioned above), so $r(Si_R)$ decreases regardless of $r(Ge_D)$. In an acid solution with an intermediate concentration (6 M), $r(Ge_D) \leq r(Si_R)$ promotes structural preservation during the treatment. At the same time, the equilibrium Si concentrations measured by ICP-MS in the mother liquors isolated after the treatment of UWY-2.6 zeolite were found to decrease from 4 to 0.3 mmol L^{-1} with the increase in HCl concentration from 0.1 to 12 M, while the Ge concentration was >10 times higher irrespective of the treatment conditions. This indicates the limited impact of equilibrium parameters (*e.g.,* solubility of framework elements) on zeolite stabilization under acidic conditions. The exchange rate between Ge and Si atoms is high when in contact with the acid solution, subsequently slowing down over time until it reaches a plateau, with no apparent change in framework composition. At high temperatures, both Si re-intercalation and the dissolution of framework Si can be further accelerated, especially in concentrated acid solutions. As a result, the products of high-temperature treatment with 12 M HCl show higher Si/Ge ratios compared to initial germanosilicates but possess mesopores, indicating the partial dissolution of the zeolite framework (Table S2†). Fig. 4 summarizes some of the mentioned aspects and potential reaction pathways during the treatment of germanosilicate zeolites under acidic conditions.

Although $2D_{D4R}$ UWY is considered less stable than most $1D_{D4R}$ materials, the decrease in the concentration of Ge atoms in D4R units allowed to reach $r(Ge_D) \leq r(Si_R)$ for this zeolite in low-concentration 0.1 M HCl, albeit at 100 °C. In contrast, $1D_{D4R}$ with a higher fraction of Ge collapsed under similar conditions suggesting that $r(Ge_D) > r(Si_R)$. Therefore, reaching $r(Ge_D) \leq r(Si_R)$ for the structural stabilization of germanosilicates may require not only optimizing treatment conditions (acid concentration and temperature), but also adjusting the chemical composition of the starting materials, especially in extremely labile structures, such as $3D_{D4R}$ zeolites, as recently

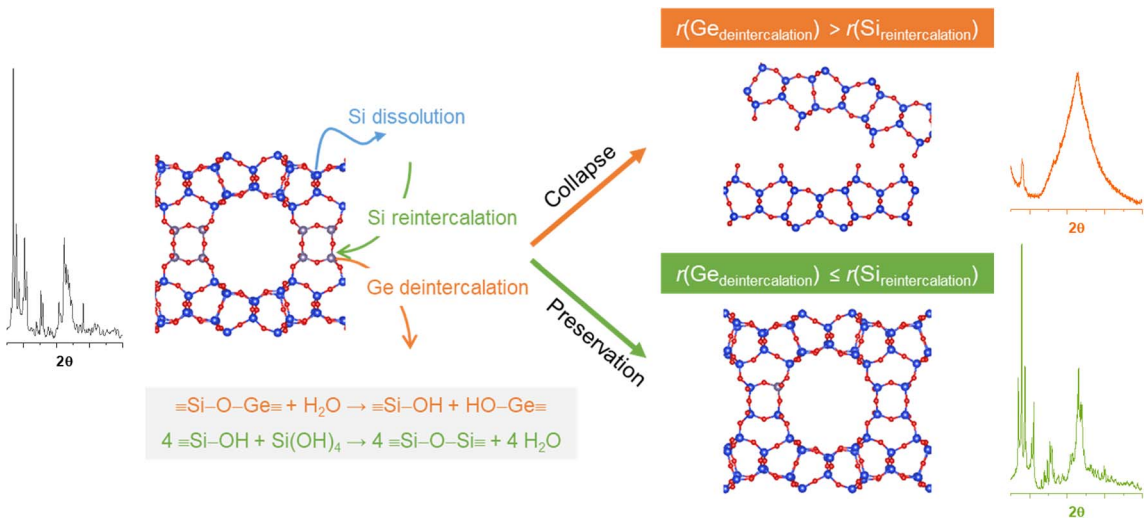

Fig. 4 Schematic representation showing the mechanism of structural reconstruction and collapse of germanosilicate zeolites in an acid solution.

 This journal is © The Royal Society of Chemistry 2024

Open Access Article. Published on 21 October 2024. Downloaded on 2/21/2026 7:51:59 PM. This article is licensed under a Creative Commons Attribution 3.0 Unported Licence.

reviewed by P. Wu *et al.*[38] Our studies showed that simply varying the stabilization conditions was insufficient to prevent the hydrolytic degradation of the $3D_{D4R}$ ITT zeolite with a typical Si/Ge ratio of 1.9. Therefore, our future efforts will be focused on optimizing the chemical composition of this $3D_{D4R}$ zeolite to make it a more suitable candidate for stabilization.

3.6. Functionalization and potential application of stabilized zeolites

Catalysis is one of the most important applications of zeolites with well-developed methods for the optimization of industry-standard aluminosilicate zeolite catalysts.[39] These include both (1) modifications of the chemical composition of the zeolite framework without considerable structural changes and (2) transformations that generate extra porosity to facilitate diffusion within zeolite particles. In contrast to aluminosilicates, the field of germanosilicate modification is still in its infancy. Currently, there are no general methods for the direct synthesis of hydrolytically stable low-concentration Ge zeolites with the studied topologies or for the indirect post-synthesis stabilization of organic-free germanosilicates, especially those with a multidimensional distribution of labile Ge-rich structural units.[40] We believe our work can help pave the way toward the rational optimization of germanosilicate properties (*i.e.*, hydrolytic stability and porosity) through post-synthesis approaches, which can be combined with incorporation of catalytically active sites and further recovery and recycling of rarely abundant Ge.[41]

As the experimental results suggest, changes in the Si/Ge ratio not only improve the hydrolytic stability of a germanosilicate zeolite (Fig. S8†) but also modify textural properties, such as the micro-to-mesopore volume ratio (Table S2†) and pore size distribution (Fig. S6, S13 and S19†). For example, low-temperature treatment with 6 M HCl increases the Si/Ge ratio in the stabilized zeolites, while maintaining the framework integrity and micropore volume. This is the preferred stabilization method for both $1D_{D4R}$ and $2D_{D4R}$ germanosilicates when the goal is to maintain the microporous character of a zeolite with a characteristic pore-size-distribution. Alternatively, high-temperature treatment with 6 M or 12 M HCl (depending on the zeolite structure) is the method of choice for developing mesoporosity (Fig. S13 and S19†). Importantly, regardless of the treatment conditions or the germanosilicate structure, the stabilized zeolites show a homogeneous distribution of the framework-building elements within their crystals (Fig. S21†). This highlights the applicability of the developed deintercalation/reinsertion approach for the preparation of chemically uniform, yet hydrolytically stable $1D_{D4R}$ and $2D_{D4R}$ zeolites.

Post-synthesis alumination of UWY-2.6 zeolite, stabilized using low-temperature treatment with 6 M HCl did not significantly alter the structural integrity of the material (Fig. S22†) or its textural properties (Fig. S23 and Table S2†), but it resulted in generation of Brønsted (the characteristic band at 1545 cm^{-1} in FTIR-Py spectra, Fig. S24†) and Lewis (the characteristic band at 1455 cm^{-1} in FTIR-Py spectra, Fig. S24†) acid sites. According to pyridine thermodesorption results, ~20% of Brønsted acid sites and ~40% of Lewis acid sites in UWY-2.6/SBZ/Al retain pyridine at 450 °C (Fig. S25†). The incorporation of these active sites led to the distinct catalytic performance of UWY-2.6/SBZ/Al in acid-catalyzed benzoylation of p-xylene. The studied reaction over zeolite catalysts may result in the formation of targeted 2,5-dimethylbenzophenone as well as side products, such as benzoic anhydride and benzoic acid (Fig. S26†). Benzoic anhydride was the only product formed over Al-free UWY-2.6 zeolite with weak Lewis acidity (Fig. S25†), similar to the blank experiment. In contrast, the UWY-2.6/SBZ/Al catalyst facilitated the formation of the targeted 2,5-dimethylbenzophenone (selectivity = 60% at conversion = 40% after 300 min, Fig. S26†), aligning with the previously reported efficiency of strong acid sites located in large pores in the Friedel–Crafts acylation.

4. Conclusions

Germanosilicate zeolites with low Si/Ge ratios, particularly in OSDA-free form and with a multidimensional population of D4R units, are highly labile and susceptible to water, undergoing structural transformation, disorder, or even collapse due to the mismatch between Ge de-intercalation ($r(Ge_D)$) and Si re-insertion ($r(Si_R)$) rates. Nevertheless, the structure of these labile zeolites in OSDA-free form can be preserved and stabilized by optimizing the post-treatment acid concentrations to control the kinetics of de-intercalation and re-insertion of framework atoms. As a case in point, the UWY structure with an adequate Si/Ge ratio is preserved when $r(Ge_D) \leq r(Si_R)$ in 6 M HCl solution at RT, but it collapses when $r(Ge_D) > r(Si_R)$. The higher hydrolytic stability of Si–O bonds compared to Ge–O enables the isomorphous substitution of Ge atoms for Si and, hence, structural maintenance in acid solution. Notwithstanding this apparent framework maintenance, dynamic changes (including structural collapse–restoration) in the chemical composition and state of the framework atoms occur upon the acidic treatment of zeolites. In addition, $r(Si_R)$ can be accelerated at high temperatures, further increasing the Si/Ge ratio of products and their structural resilience over a broader range of acid concentrations.

Since the impact of stabilization conditions on the framework integrity and related textural properties is substantial, the developed approach can be used for the preparation of micro- or micro-mesoporous zeolites, showing distinct catalytic behavior after the incorporation of active sites. Thus, isomorphous substitution combined with the recovery and recycling of rarely abundant germanium is considered a viable way to use the unique structural characteristics of stabilized germanosilicate zeolites in catalytic applications.

Our stabilization strategy is reliable not only for UWY with Ge-enriched D4R units propagating in two directions but also for many other germanosilicate zeolites containing D4R units propagating along one crystallographic axis, including ITR, IWV, and *CTH. Collectively, our findings demonstrate that labile germanosilicates zeolites can yield products with a high Si/Ge ratio suitable for prospective applications or further modifications of their chemical properties.

Open Access Article. Published on 21 October 2024. Downloaded on 2/21/2026 7:51:59 PM.
This article is licensed under a Creative Commons Attribution 3.0 Unported Licence.

Data availability

The data supporting this article have been included as part of the ESI.†

Author contributions

J. Z.: conceptualization; investigation (synthesis, post-synthesis, and XRD measurements); formal analysis; writing – original draft. Q. Y.: conceptualization; investigation (synthesis and XRD and physisorption measurements); formal analysis; writing – original draft. E. S.: investigation (supplementary synthesis and post-synthesis, functionalization, catalytic tests, and XRD and SEM measurements); formal analysis. S. A.: investigation (supplementary post-synthesis and XRD measurements); formal analysis. O. P.: investigation (NMR measurements); formal analysis. J. Č.: supervision; writing – review & editing. S. M.: supervision; writing – review & editing. M. O.: conceptualization; supervision; writing – review & editing. M. S.: conceptualization; supervision; project administration; funding acquisition; writing – review & editing. All authors contributed to the final version of the manuscript.

Conflicts of interest

The authors declare that they have no conflict of interest.

Acknowledgements

The authors thank Dr M. Kubů for ICP-MS analysis. This research was funded by the Ministry of Education, Youth and Sports of Czech Republic through the ERC_CZ project LL 2104 (E. S., O. P., M. S., and M. O.). The authors acknowledge the Charles University Centre of Advanced Materials (CUCAM – OP VVV Excellent Research Teams, no. CZ.02.1.01/0.0/0.0/15_003/0000417) for providing infrastructure enabling this research. The authors acknowledge the Viničná Microscopy Core Facility (VMCF of the Faculty of Science, Charles University), a facility supported by Ministerstvo Školství, Mládeže a Tělovýchovy (LM2023050 Czech-BioImaging), for their assistance with microscopy. The authors thank Dr Carlos V. Melo for editing the manuscript.

References

1 V. Van Speybroeck, K. Hemelsoet, L. Joos, M. Waroquier, R. G. Bell and C. R. A. Catlow, Advances in theory and their application within the field of zeolite chemistry, *Chem. Soc. Rev.*, 2015, **44**, 7044–7111.
2 J. Li, A. Corma and J. Yu, Synthesis of new zeolite structures, *Chem. Soc. Rev.*, 2015, **44**, 7112–7127.
3 A. Corma, M. T. Navarro, F. Rey, J. Rius and S. Valencia, Pure polymorph C of zeolite beta synthesized by using framework isomorphous substitution as a structure-directing mechanism, *Angew. Chem., Int. Ed.*, 2001, **40**, 2277–2280.
4 J. L. Paillaud, Y. Lorgouilloux, B. Harbuzaru, P. Caullet, J. Patarin and N. Bats, in *Stud. Surf. Sci. Catal.*, ed. R. Xu, Z. Gao, J. Chen and W. Yan, Elsevier, 2007, vol. 170, pp. 389–396.
5 P. Kamakoti and T. A. Barckholtz, Role of germanium in the formation of double four rings in zeolites, *J. Phys. Chem. C*, 2007, **111**, 3575–3583.
6 H. Xu, J. Jiang, B. Yang, H. Wu and P. Wu, Effective Baeyer–Villiger oxidation of ketones over germanosilicates, *Catal. Commun.*, 2014, **55**, 83–86.
7 X. Hou, Z. Yao, H. Li, M. Wang, Y. Wei, L. Zhang, Y. Liang, J. Qiao, J. Jia and R. Zhang, Tailored alkyl-imidazolium templating synthesis of extra-large-pore germanosilicate zeolite ITT as Baeyer-Villiger oxidation catalyst, *Microporous Mesoporous Mater.*, 2023, **348**, 112340.
8 I. Podolean, J. Zhang, M. Shamzhy, V. I. Pârvulescu and J. Čejka, Solvent-free ketalization of polyols over germanosilicate zeolites: the role of the nature and strength of acid sites, *Catal. Sci. Technol.*, 2020, **10**, 8254–8264.
9 M. Trachta, T. Volný, R. Bulánek, E. Koudelková, J. Halamek, M. Rubeš, M. Shamzhy, M. Mazur, J. Čejka and O. Bludský, Strong CO_2 adsorption in narrow-pore ADOR zeolites: A combined experimental and computational study on IPC-12 and related structures, *J. CO2 Util.*, 2023, **74**, 102548.
10 A. Zukal, M. Shamzhy, M. Kubů and J. Čejka, The effect of pore size dimensions in isoreticular zeolites on carbon dioxide adsorption heats, *J. CO2 Util.*, 2018, **24**, 157–163.
11 M. O'Keeffe and O. M. Yaghi, Germanate zeolites: Contrasting the behavior of germanate and silicate structures built from cubic T_8O_{20} units (T=Ge or Si), *Chem.–Eur. J.*, 1999, **5**, 2796–2801.
12 M. Jin, O. Veselý, C. J. Heard, M. Kubů, P. Nachtigall, J. Čejka and L. Grajciar, The role of water loading and germanium content in germanosilicate hydrolysis, *J. Phys. Chem. C*, 2021, **125**, 23744–23757.
13 P. Chlubná-Eliášová, Y. Tian, A. B. Pinar, M. Kubů, J. Čejka and R. E. Morris, The Assembly-Disassembly-Organization-Reassembly Mechanism for 3D-2D-3D Transformation of Germanosilicate IWW Zeolite, *Angew. Chem., Int. Ed.*, 2014, **53**, 7048–7052.
14 P. Eliášová, M. Opanasenko, P. S. Wheatley, M. Shamzhy, M. Mazur, P. Nachtigall, W. J. Roth, R. E. Morris and J. Čejka, The ADOR mechanism for the synthesis of new zeolites, *Chem. Soc. Rev.*, 2015, **44**, 7177–7206.
15 J. Jiang, J. L. Jorda, M. J. Diaz-Cabanas, J. Yu and A. Corma, The synthesis of an extra-large-pore zeolite with double three-ring building units and a low framework density, *Angew. Chem., Int. Ed.*, 2010, **49**, 4986–4988.
16 D.-R. Liu, Z.-H. Gao, W.-W. Zi, J. Zhang, H.-B. Du and F.-J. Chen, Facile synthesis of large-pore zeolite ITQ-26 by using an easily-available imidazolium as structure-directing agent, *Microporous Mesoporous Mater.*, 2019, **276**, 232–238.
17 W. J. Roth, P. Nachtigall, R. E. Morris, P. S. Wheatley, V. R. Seymour, S. E. Ashbrook, P. Chlubná, L. Grajciar, M. Položij, A. Zukal, O. Shvets and J. Čejka, A family of zeolites with controlled pore size prepared using a top-down method, *Nat. Chem.*, 2013, **5**, 628–633.

 This journal is © The Royal Society of Chemistry 2024

Open Access Article. Published on 21 October 2024. Downloaded on 2/21/2026 7:51:59 PM.
This article is licensed under a Creative Commons Attribution 3.0 Unported Licence.

18 M. Opanasenko, M. Shamzhy, F. Yu, W. Zhou, R. E. Morris and J. Čejka, Zeolite-derived hybrid materials with adjustable organic pillars, *Chem. Sci.*, 2016, **7**, 3589–3601.
19 M. Shamzhy, M. Mazur, M. Opanasenko, W. J. Roth and J. Čejka, Swelling and pillaring of the layered precursor IPC-1P: tiny details determine everything, *Dalton Trans.*, 2014, **43**, 10548–10557.
20 H. Xu, J.-G. Jiang, B. Yang, L. Zhang, M. He and P. Wu, Post-synthesis treatment gives highly stable si†liceous zeolites through the isomorphous substitution of silicon for germanium in germanosilicates, *Angew. Chem., Int. Ed.*, 2014, **53**, 1355–1359.
21 F. Gao, M. Jaber, K. Bozhilov, A. Vicente, C. Fernandez and V. Valtchev, Framework stabilization of Ge-rich zeolites *via* postsynthesis alumination, *J. Am. Chem. Soc.*, 2009, **131**, 16580–16586.
22 Y. Zhou, S. A. Kadam, M. Shamzhy, J. Čejka and M. Opanasenko, Isoreticular UTL-Derived Zeolites as Model Materials for Probing Pore Size–Activity Relationship, *ACS Catal.*, 2019, **9**, 5136–5146.
23 M. V. Shamzhy, P. Eliašová, D. Vitvarová, M. V. Opanasenko, D. S. Firth and R. E. Morris, Post-Synthesis Stabilization of Germanosilicate Zeolites ITH, IWW, and UTL by Substitution of Ge for Al, *Chem.–Eur. J.*, 2016, **22**, 17377–17386.
24 M. V. Shamzhy, M. V. Opanasenko, F. S. d. O. Ramos, L. Brabec, M. Horáček, M. Navarro-Rojas, R. E. Morris, H. d. O. Pastore and J. Čejka, Post-synthesis incorporation of Al into germanosilicate ITH zeolites: the influence of treatment conditions on the acidic properties and catalytic behavior in tetrahydropyranylation, *Catal. Sci. Technol.*, 2015, **5**, 2973–2984.
25 P. S. Wheatley, P. Chlubná-Eliášová, H. Greer, W. Zhou, V. R. Seymour, D. M. Dawson, S. E. Ashbrook, A. B. Pinar, L. B. McCusker, M. Opanasenko, J. Čejka and R. E. Morris, Zeolites with continuously tuneable porosity, *Angew. Chem., Int. Ed.*, 2014, **53**, 13210–13214.
26 S. Abdi, M. Kubů, A. Li, K. Kalíková and M. Shamzhy, Addressing confinement effect in alkenes epoxidation using 'isoreticular' titanosilicate zeolite catalysts, *Catal. Today*, 2022, **390–391**, 326–334.
27 J. Zhang, O. Veselý, Z. Tošner, M. Mazur, M. Opanasenko, J. Čejka and M. Shamzhy, Toward controlling disassembly step within the ADOR process for the synthesis of zeolites, *Chem. Mater.*, 2021, **33**, 1228–1237.
28 S. E. Henkelis, M. Mazur, C. M. Rice, P. S. Wheatley, S. E. Ashbrook and R. E. Morris, Kinetics and mechanism of the hydrolysis and rearrangement processes within the assembly–disassembly–organization–reassembly synthesis of zeolites, *J. Am. Chem. Soc.*, 2019, **141**, 4453–4459.
29 M. Shamzhy and F. S. D. Ramos, Tuning of acidic and catalytic properties of IWR zeolite by post-synthesis incorporation of three-valent elements, *Catal. Today*, 2015, **243**, 76–84.
30 M. Dodin, J.-L. Paillaud, Y. Lorgouilloux, P. Caullet, E. Elkaim and N. Bats, A zeolitic material with a three-dimensional pore system formed by straight 12- and 10-ring channels synthesized with an imidazolium derivative as structure-directing agent, *J. Am. Chem. Soc.*, 2010, **132**, 10221–10223.
31 M. Peng, J. Jiang, X. Liu, Y. Ma, M. Jiao, H. Xu, H. Wu, M. He and P. Wu, Breaking structural energy constraints: Hydrothermal crystallization of high-silica germanosilicates by a building-unit self-growth approach, *Chem.–Eur. J.*, 2018, **24**, 13297–13305.
32 Y. Ji, Y. Wang, B. Xie and F.-S. Xiao, Zeolite seeds: Third type of structure directing agents in the synthesis of zeolites, *Comments Inorg. Chem.*, 2016, **36**, 1–16.
33 X. Liu, U. Ravon, F. Bosselet, G. Bergeret and A. Tuel, Probing Ge Distribution in Zeolite Frameworks by Post-Synthesis Introduction of Fluoride in As-Made Materials, *Chem. Mater.*, 2012, **24**, 3016–3022.
34 A. Rodríguez-Fernández, F. J. Llopis, C. Martínez, M. Moliner and A. Corma, Increasing the stability of the Ge-containing extra-large pore ITQ-33 zeolite by post-synthetic acid treatments, *Microporous Mesoporous Mater.*, 2018, **267**, 35–42.
35 X. Liu, W. Mao, J. Jiang, X. Lu, M. Peng, H. Xu, L. Han, S.-a. Che and P. Wu, Topotactic Conversion of Alkali-Treated Intergrown Germanosilicate CIT-13 into Single-Crystalline ECNU-21 Zeolite as Shape-Selective Catalyst for Ethylene Oxide Hydration, *Chem.–Eur. J.*, 2019, **25**, 4520–4529.
36 J. H. Kang, D. Xie, S. I. Zones, S. Smeets, L. B. McCusker and M. E. Davis, Synthesis and Characterization of CIT-13, a Germanosilicate Molecular Sieve with Extra-Large Pore Openings, *Chem. Mater.*, 2016, **28**, 6250–6259.
37 O. Veselý, P. Eliášová, R. E. Morris and J. Čejka, Reverse ADOR: reconstruction of UTL zeolite from layered IPC-1P, *Adv. Mater.*, 2021, **2**, 3862–3870.
38 M. Peng, Y. Zhao, H. Xu, J. Jiang and P. Wu, Double Four Ring Units-Containing Zeolites: Synthesis, Structural Modification and Catalytic Applications, *Chem.–Eur. J.*, 2024, **30**, e202303657.
39 V. Valtchev, G. Majano, S. Mintova and J. Pérez-Ramírez, Tailored crystalline microporous materials by post-synthesis modification, *Chem. Soc. Rev.*, 2013, **42**, 263–290.
40 M. Opanasenko, M. Shamzhy, Y. Wang, W. Yan, P. Nachtigall and J. Čejka, Synthesis and post-synthesis transformation of germanosilicate zeolites, *Angew. Chem., Int. Ed.*, 2020, **59**, 19380–19389.
41 J. Zhang, Q. Yue, M. Mazur, M. Opanasenko, M. V. Shamzhy and J. Čejka, Selective Recovery and Recycling of Germanium for the Design of Sustainable Zeolite Catalysts, *ACS Sustainable Chem. Eng.*, 2020, **8**, 8235–8246.